XVII IAHR SYMPOSIUM
Beijing, China 1994

MECHANISM OF THE EFFICIENCY DROP DUE TO TRAVELING BUBBLE CAVITATION

Christophe Arn, François Avellan, Pierre Henry
IMHEF - EPF Lausanne - Switzerland

ABSTRACT

The setting level of a hydraulic machine, specially for low head machines, is decided with respect to the possible alteration of the efficiency due to the cavity development. In the case of traveling bubble cavitation, corresponding to the outlet cavitation at the nominal head, the physical phenomenon underlying such an efficiency alteration is not very clear, even though a strong dependence of this drop with the volume of cavities have ben noticed. The aim of this paper is to present the results of an experiment intending to explain physically the influence of bubble cavitation on the performance of a hydraulic profile.

RESUME

L'implantation d'une turbine hydraulique et plus particulièrement celle des machines à hautes chutes, est définie en fonction de l'altération possible du rendement due au développement de cavitation. Dans le cas de la cavitation à bulles, apparaissant à la sortie de l'aubage à la chute nominale, les phénomènes physiques provoquant cette baisse de rendement ne sont pas clairement expliqués même si on montre une dépendance certaine entre l'altération deu rendement et le volume des cavités. Le sujet de ce papier est la présentation des résultats d'une manipulation expérimentale réalisée dans le but d'expliquer physiquement l'influence de la cavitation à bulles sur les performances d'un profil hydraulique.

1. Introduction

Traveling bubble cavitation takes place for the design value of the head, at the throat of the runner flow passage, close to the outlet and corresponds to low flow angle of attack. This type of cavitation is very sensitive to the content of cavitation nuclei and to the value of the setting level. For this reason, this setting level is determined with respect to this type of cavitation. The physical phenomenon underlying such an efficiency alteration of the turbine is not yet very clear. Previous experiments [2] performed with a NACA 009 profile equiped with a hydrodynamic balance show us the hydrodynamic loads to be dependant on the cavitation coefficient σ and the content of the cavitation nuclei, as shown on Figure 1.

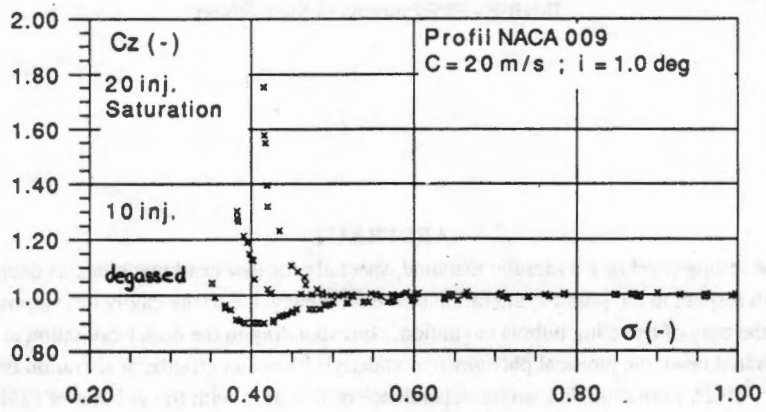

Figure 1: Lift coefficient in function of σ and nuclei rate (number of injectors).

We can observe that the lift coefficient increases for low values of σ and for high values of cavitation nuclei rate. Since the lift is generated by the pressure repartition on the blade, we can deduct that these are responsible for that pressure modification on the profile. An approach to study this influence is to consider traveling bubble like a non moving sphere in expansion in a still fluid. Indeed, the relative velocity between the bubble and the fluid is very low. The potential theory of incompressible flows allows to class this case as the determination of the pressure generated by a potential Φ wich is given by

$$\Phi = -\dot{R}R^2 r^{-1} \qquad [m^2/s]$$

where R is the radius of the sphere [1]. The expansion of this sphere generate a radial pressure field around. The Bernoulli equation leads to the following expression of the pressure field p where p_∞ is far field pressure, C the velocity and ρ the water density.

$$p_\infty = \left[p + \frac{1}{2}\rho(C^2) + \rho\frac{\partial \Phi}{\partial t} \right] \quad \text{[Pa]}$$

The instaneous pressure generated onto a plane at a distance d from the center of the sphere is obtained by the following relation

$$p(x) = p_\infty + \rho\left(\frac{\ddot{R}R^2 + 2\dot{R}^2 R}{\sqrt{x^2 + d^2}} - \frac{1}{2}\left(\frac{\dot{R}R^2}{x^2 + d^2} \right)^2 \right) \quad \text{[Pa]}$$

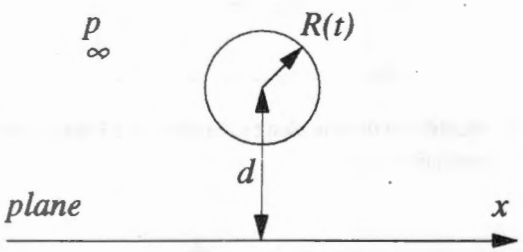

Figure 2: Expansion of a sphere in a still fluid.

Thus, the pressure on the blade can be obtained approximately by superposing two bubble potential fields according to the image superposition technique if the evolution of the radius $R(t)$ is known. The Rayleigh-Plesset model allows us to determine this evolution in an external and variable pressure field. In the case of a Francis turbine of specific velocity ν=0.27, whose pressure field is computed by a 3D potential finite element code, the evolution of bubbles along streamlines on the blade is determined by a Rayleigh-Plesset code based on the Runge-Kutta method [2], [7]. One can see these evolutions on Figure 3. For a value of x/L , we can determine R, $\dot{R}$, $\ddot{R}$ and then the value of the generated pressure on the wall, (see Figure 4).

The aim of this paper is to verify the validity of this approach by comparing the bubble size and pressure wall measurements in a bidimensional profile NACA 009 to these calculations.

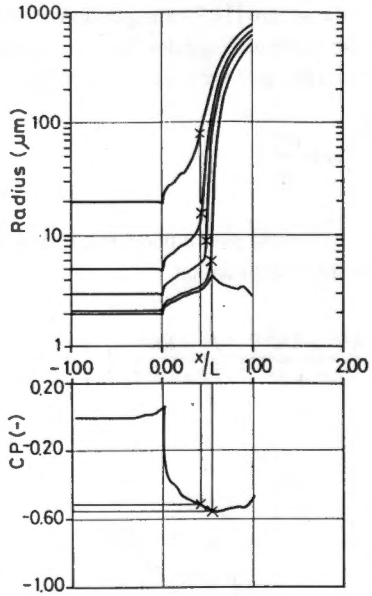

Figure 3: Bubbles evolution along streamline in a Francis turbine at nominal operation point.

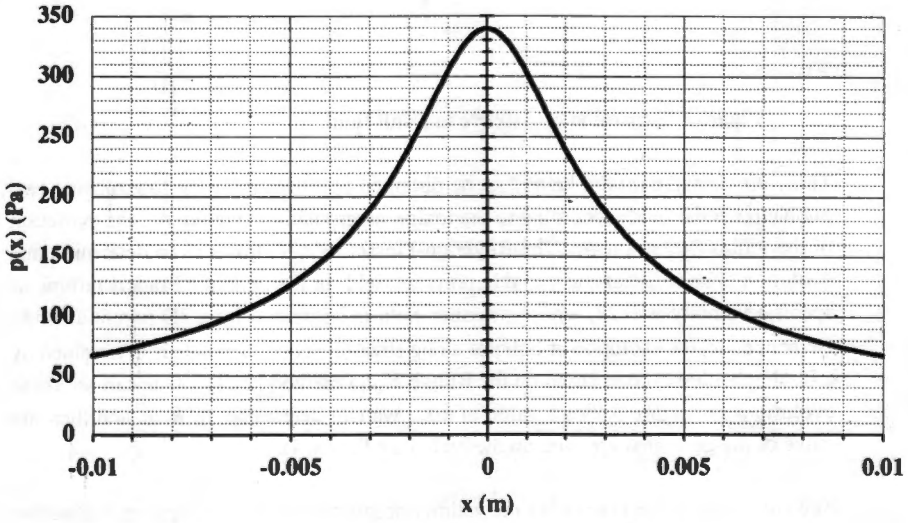

Figure 4: Pressure generated by an exploding bubble on a wall located at distance of 1mm of this center. *x/L=0.5*.

2. Experimental Set-Up

2.1 Pressure Instrumentation

The tests are carried out in the IMHEF high speed cavitation tunnel [3]. The experimental hydrofoil is a 2D NACA009, 100 mm long and 150 mm wide, truncated at 90 % of its length [4]. 30 piezoresistive absolute pressure transducers are distributed on the suction side of the blade, Figure 5. The measurement range covers 0 to 200 bar. Each transducer is supplied by an independant current source and its output pressure signal is separatly amplified and band-pass filtered. Data acquisition is performed with the help of two digital transient recorders with a 12 bits resolution per sample. The first one (LeCroy 8212a) allows simultaneous data acquisition of 32 signals at a maximum sampling frequency of 5 kHz whereas the second one ensures simultaneous data acquisition of 12 channels at a maximum sampling rate of 1 MHz (3 modules LeCroy 6810).

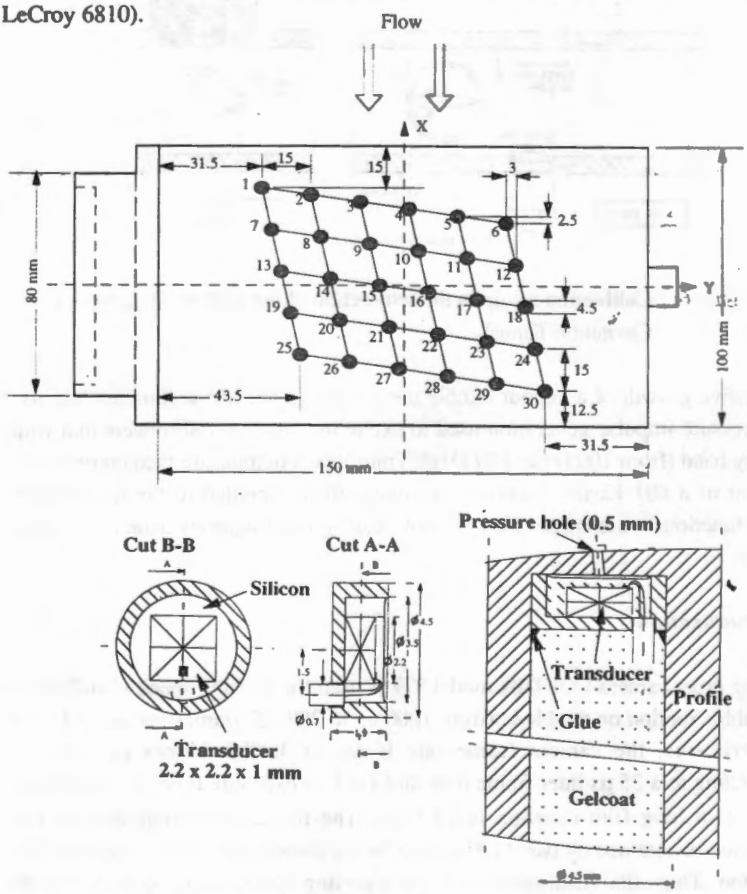

Figure 5: NACA009 hydrofoil equipped with 30 transient pressure transducers. Pressure transducer mounting.

2.2 Pressure calibration

Static calibration of the pressure transducers is performed with the blade mounted in the test section by varying the static pressure in the tunnel from 0.1 to 10 bar (Figure.6). To achieve a dynamic calibration of the pressure transducers, a special technique is developed to generate a pressure impulse in the test section [5]. A discharge of 5 to 50 J electric energy is performed through coaxial probes previously introduced in the test section. The use of a high speed switch allows a discharge duration ranging from 5 to 20 μs.

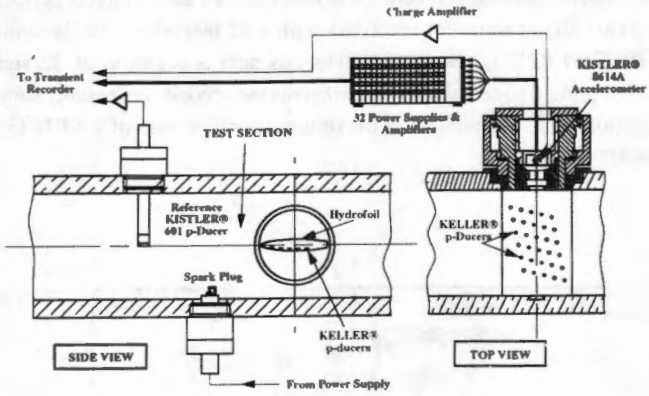

Figure 6: Calibration set-up in the test section of the IMHEF High Speed Cavitation Tunnel

An explosive growth of a vapour bubble takes place in the test section leading to a strong pressure impulse generation used to excite the pressure transducers in a wide frequency band (from 100 Hz to 100 kHz). Transducers outputs are then compared to the output of a 601 Kistler pressure transducer flush mounted to the test section. Transfer functions are averaged over 32 shots leading to a frequency band in the range 0-30 kHz.

2.3 Visualization

A rotating drum camera CORDIN model 377 is used for the high speed visualisation of the bubble motion on the blade (from 1000 up to 200'000 frames per second). For the experiments, the camera frame rate is set to 40'000 frames per second, corresponding to a 25 μs inter frame time and a 4.1 μs exposure time. For this frame rate, the 1 m long film duration is 12.5 ms. The illumination required for this visualisation is obtained by two 1100 J flash lamps placed at the side window of the test section. Thus, the visualisations of the traveling bubbles on the blade can be carried out across the top window of the test section. Transient pressure measurements are performed simultaneously with high speed visualisations.

2.4 Nuclei injector

The micro-bubbles injection [6] system is composed of two parts, the first consists of the continuous production of air-saturated water and the other one is concerned with the actual generation and injection of cavitation nuclei (see Figure 7). The saturation of the water with air is obtained by producing a water spray at high pressure, 10 to 30 bar. The nuclei are generated by a sudden expansion of the air-saturated water through a serie of injection modules. Each injection module supplies a fixed quantity of cavitation nuclei. By varying the number of injection modules one can obtain the required quantity of cavitation nuclei in the test section.

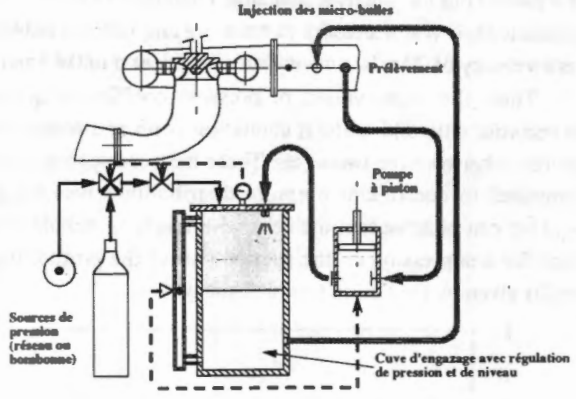

Figure 7: The micro-bubbles injection system.

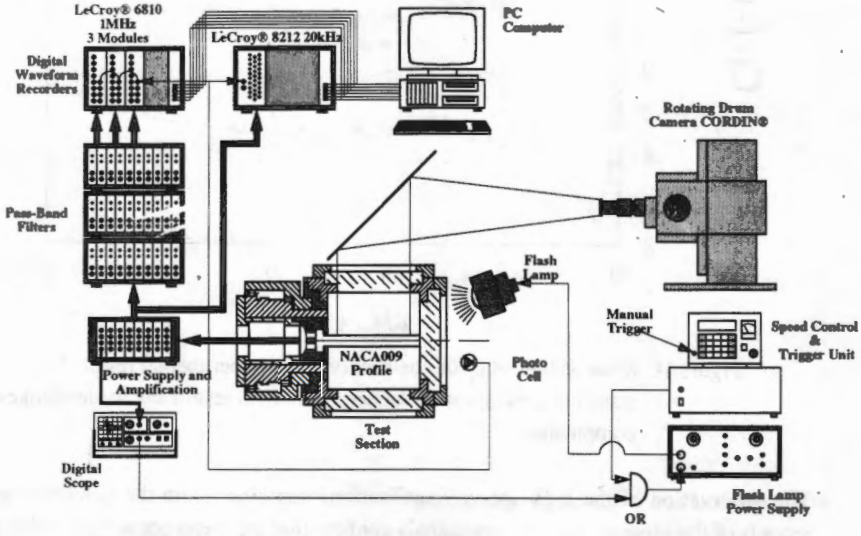

Figure 9: Experimental set-up

2.5 Experimental set-up

Simultaneous measurements required accurate sequence for the starting of all the instruments. To be sure that the high speed visualisation contains at least one traveling bubble, the first trigger signal comes from the pressure transducer closest to the leading edge of the blade. The combination of this signal and the camera shutter opening triggers the flash lamps. Then a 1 ns rise time photo diode, EG&G FND100, detects the flash light and triggers the transient recorders (Figure 9).

3. Results and discussions

The tests are carried out for one hydrodynamic condition. Indeed, to obtain good high-speed visualisations, it was necessary to have big and isolated bubbles. The choosen condition is a velocity of 20 m/s, a cavitation coefficient σ of 0.43 and for an incidence angle of 1°. Then, the mean values of pressure coefficient c_p measured by low frequences recorder with and without cavitation (with and without nuclei injection) show a difference between the two cases. These measurements are reported on Figure 10 and compared to coefficient pressure distribution given by a Navier-Stokes calculation. One can observe that the case with traveling bubble cavitation shows a upward trend for a depression on the suction side of the profile. It is in accordance with the results given by the hydrodynamic balance.

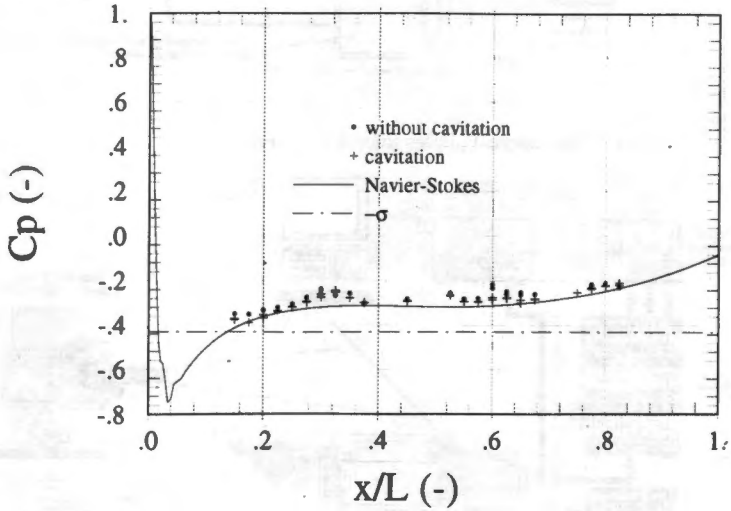

Figure 10: Mean values of c_p on the suction side. Experimental results by transient pressure transducers. Numerical results by Navier-Stokes computation

The observation of the high-speed visualisations combined with the simultaneous records of the pressure transducers signals confirm that the mean pressure is reduced

by traveling bubble cavitation occurence. One can observe on Figure 11 and 12 that the passage of the cavities above the transducers corresponds to a pressure drop beside the mean pressure (transducer n°3, before and after t=18 ms and tranducer n°9, t=19 ms).

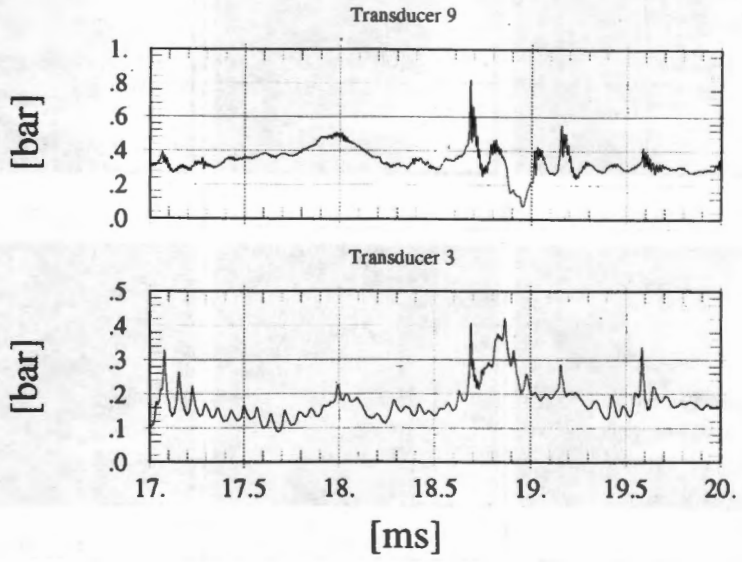

Figure 11: Pressure signals from transducers n°3 and n°9

These results can be qualitatively explained by the theory already introduced. Indeed, for the choosen hydrodynamic condition, all the transducers are in a zone where the size of the bubbles is relatively stable or decreasing. If we apply our approach, we can observe in Figure 14 that the pressure generated by the expansion of the bubble located 2 mm above the blade is positive until a x/L value of 0,105. To perform this calculation, we have used the bubble radius as well as it first and second derivatives along the blade chord given by image processing of the high-speed visualisation. This measured evolution of the bubble radius along the profile is reported on Figure 13. Moreover, we can see on Figure 14 that the pressure goes up again in the zone close to a value $x/L=0.3$. This is the zone of the collapses and the rebounds and the pressures generated are very instationnary. This can explain the appearance of the pressure signal from the transducer n°9 at the moment of the collapse of the bubble seen in the high-speed visualisation (19 ms, Figure 11 and 12).

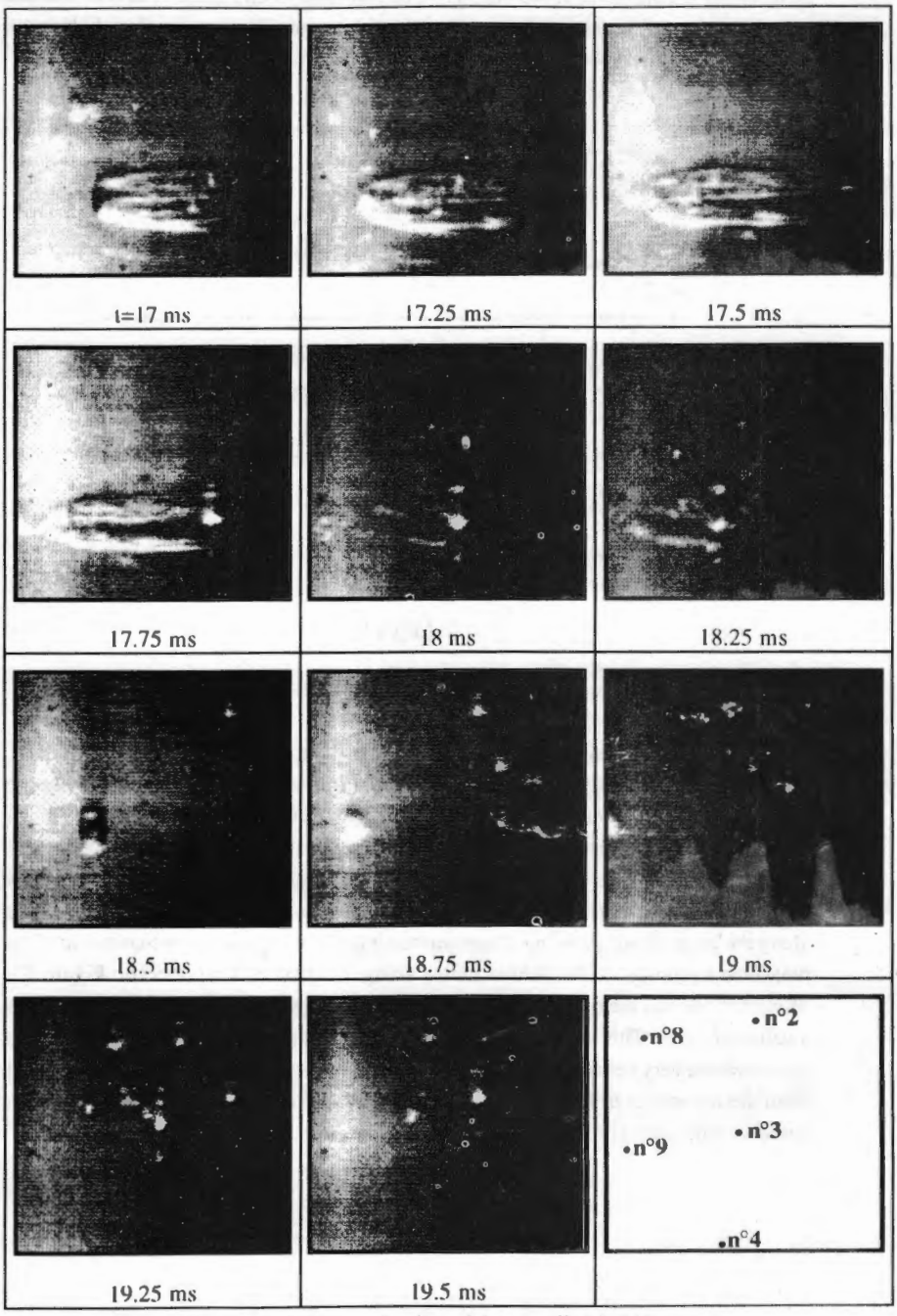

Figure 12: High-speed visualisation of the traveling bubbles

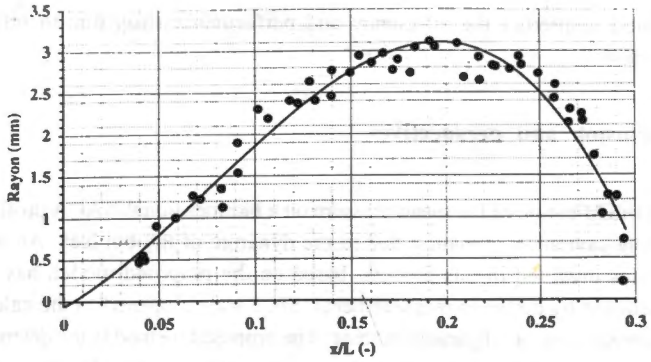

Figure 13: Bubble radius evolution measured along the NACA009 profile

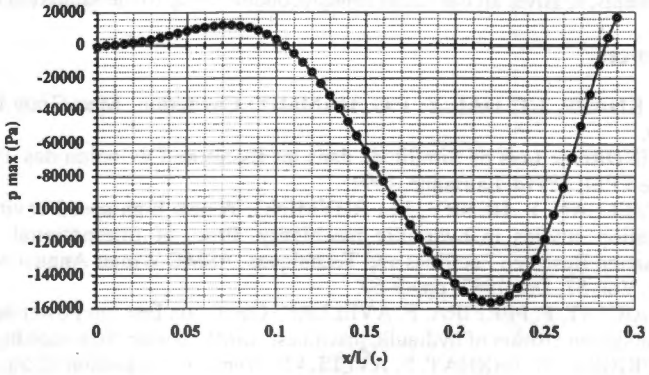

Figure 14: Pressure generated by the expansion of the bubbles along the NACA009 profile.

The pressure pulses generated by the traveling bubbles can be transduced in term of mean pressure coefficient. Then, the next step is to correct the coefficient pressure distribution without cavitation adding the mean pressure coefficient distribution generated by the bubbles. If the choosen approach is correct, the following relation should be verified

$$c_{P\,whit\ cavitation} = c_{P\,whitout\ cavitation} + K(Nuclei\ rate)c_{P\,bubbles}$$

and then the lift with cavitation can be determined by integration. We can observe with our results that this relation is not verified all along the blade chord. Moreover, the distance between the bubble and the blade varies along the profile and the boundary layer effects are not included in this model. However, this approach, based on a expansion of the bubbles is certainly a good way for the elaboration of a calculation

method to predict the efficiency and performance drop due to traveling bubble cavitation.

4. Conclusion and perspectives

The modification of the mean pressure on a bidimensional NACA profile by traveling bubble cavitation is mainly due to the dynamic of the bubbles. An analysis of the physics involved in this process, based on the proposed model, has been partially confirmed by different measurements. So, a way is opened to the calculation of the efficiency drop of a hydraulic turbine. The proposed method is the determination of the modification the mean coefficient pressure distribution whitout cavitation due to contribution of the pressure pulses generated by the traveling bubbles. The perpectives of this work are an enhancement of the present model, as well as additional experiments, to cover all the nuclei content conditions, up to the saturation condition.

5. References

[1] R.T. KNAPP, J.T. DAILY, F.G. HAMMIT: Cavitation. Mac Graw hill, New-York, 1970.

[2] B. GINDROZ: Lois de Similitude dans les Essais de Cavitation des Turbines Francis. Thèse EPFL n°914, Lausanne, 1991.

[3] F. AVELLAN, P. HENRY, I.L. RHYMING: A new high speed cavitation tunnel for cavitation studies in hydraulic machinery. Proc. of International Symposium on Cavitation Research Facilities and Techniques, ASME Winter Annual Meeting, Boston, FED: Vol. 57, Dec 1987, pp 49-60.

[4] M. FARHAT, F. PEREIRA, F. AVELLAN: Cavitation Erosion Power as a scaling factor for cavitation erosion of hydraulic machines, ASME Winter Ann. meeting, 1993.

[5] F. PEREIRA, M. FARHAT, F. AVELLAN: Dynamic calibration of transient sensors by spark generated cavity. Proc. of Symposium on Bubble Dynamics and Interface Phenomena, IUTAM meeting, Birmingham (UK), September 1993.

[6] C. BRAND, F. AVELLAN, P. HENRY: The IMHEF system for cavitation nuclei injection. 16th Symposium of the IAHR section on Hydraulic Machinery, Sao Paolo, 1992.

[7] F. AVELLAN, P. HENRY: Theoritical and Experimental study of the inlet and outlet cavitation in a model of Francis turbine. Proc. of 12th IARH Symposium on Hydraulic Machinery in the Energy Related Industries, paper 1-3, pp 38-55, Stirling, August 1984.

[8] F. AVELLAN, Cavitation tests of hydraulic machines: Procedure and Instrumentation. ASME Winter Ann. meeting, 1993

6. Acknowledgments

The authors are particularly grateful to the members of the IMHEF Cavitation Research Group. This research is financially supported by the Swiss Federal "Commission d'Encouragement à la Recherche Scientifique", the Swiss Energy Producers Association "National Energie Forschung Fonds", Hydro Vevey and Sulzer Brothers.